

Dynamical Studies of Suprathermal Electron Relaxation by Modulated ECCD

S. Coda, S. Alberti, P. Blanchard¹, I. Klimanov, J.-M. Moret, P. Weber

*Centre de Recherches en Physique des Plasmas
Association EURATOM-Confédération Suisse
Ecole Polytechnique Fédérale de Lausanne, CRPP - EPFL, CH-1015 Lausanne, Switzerland*

1. Introduction

The relaxation phenomena governing the behaviour of suprathermal electrons largely determine the physics of electron cyclotron current drive (ECCD). Experimental and modeling work performed on TCV in recent years [1,2] has shown that both rf and collisional diffusion in velocity space and cross-field transport in physical space operate on comparable time scales, and that the latter in particular plays a key role in regulating the current profile and, at the high power levels of TCV, the current drive efficiency as well. Recent perturbative studies of the response of high field side (HFS) electron cyclotron emission (ECE) to short, low duty cycle, periodic, localised ECCD pulses have yielded promising initial quantitative results on the relaxation dynamics, which are discussed in this paper.

The TCV tokamak ($R=0.88$ cm, $a=0.25$ cm, $I_p < 1$ MA, $B_T < 1.54$ T) is equipped with a 4.5 MW, second and third harmonic EC heating system that includes 7 separate launchers, whose injection angles are adjustable in real time [3]. A second harmonic X-mode ECE radiometer, operating in the 78-114 GHz range with 24 channels of 0.75 GHz bandwidth [4], was employed in this study on either of two horizontal viewlines on the HFS [1].

2. Methodology

The ECCD pulses are applied with one or two 0.45 MW sources (with identical aiming) and are defined by a 0.2 ms ramp-up, a 0.25 ms flat top and a 0.1 ms ramp-down, with a periodicity of 8 to 10 ms. The pulse length has been empirically adjusted to be well below the time for quasilinear saturation and to permit observation of the spatial propagation of the pulse after turn-off. Coherent averaging of the ECE signals is performed throughout the steady-state phase of the discharge, comprising up to 200 pulses. This permits the pulse to be detected with good signal-to-noise ratio on all channels in spite of a modest average power (< 40 kW). The sensitivity of the measurement during the decay phase is primarily limited by the residual saw-tooth oscillations, statistically attenuated by averaging. The suprathermal origin of the signal is confirmed by a direct comparison with the signal detected by a new 65-100 GHz radiometer placed symmetrically on the low field side (LFS): the two are in excellent agreement before the pulse, whereas the HFS radiative temperature increase during the pulse is over 5 times larger than its LFS counterpart at all locations.

1. Current address: DRFC, CEA/Cadarache, 13108 Saint Paul-lez-Durance Cédex, France

To quantify the suprathermal population, we postulate a bi-Maxwellian energy distribution, with a characteristic temperature T_s and density n_s . We further assume, for this initial analysis, that T_s is independent of position. The suprathermal emission is relativistically downshifted by $\delta f/f \sim -7/4 T_s/(m_e c^2)$ [5]. This downshift can be estimated in many cases by associating the frequency of the symmetry point in the signal distribution with the point of smallest minor radius along the chord. The characteristic energy can also be independently estimated by equating the pulse decay time with the collisional slowing-down time. The two calculations are found to be in good agreement. Once an approximate value for T_s is thus obtained, the optical thickness τ_s of the suprathermal component can be derived from the expression [4] $T_{\text{rad}} = T_{\text{rad,b}} \exp(-\tau_s) + T_s [1 - \exp(-\tau_s)]$, where T_{rad} denotes the measured radiative temperature on the HFS and $T_{\text{rad,b}}$ the radiative temperature of the bulk. Finally, for a sufficiently narrow emissivity shape function, the suprathermal density can be extracted through the formula [5] $\tau_s = 3.71 n_s T_s R/B$ [10^{19} m^{-3} , keV, m, T], where R and B are the major radius and magnetic field, respectively, at the emissivity peak location. In this entire study $\tau_s < 1$, i.e. the suprathermal population is found to be optically thin, a consequence of the low average applied power.

3. Results

The time history for the reference case is shown in Fig. 1. Here, the plasma was centred in the vacuum vessel and heated centrally by one source from the LFS on the midplane, with the ECE viewline also on the midplane. The outward propagation of the pulse is clearly visible. A temperature $T_s \sim 11.5$ keV is inferred from the signal distribution, consistent with decay times of the order of 0.2-0.3 ms.

A simple measure of the radial propagation of the pulse is the time to peak (calculated from the power turn-off time), which is plotted in Fig. 2 for four different shots with increasing vertical distance between the magnetic axis and the ECE chord, and the microwave beam(s) always trained on the former. The abscissa for each shot is the emission location of downshifted radiation at $T_s = 11.5$ keV. The overlapping data are in satisfactory agreement, with most of the scatter attributed to density variations. The ray tracing code TORAY-GA [6] places the EC deposition in the region $\rho = 0-0.2$, which is confirmed by the measurements to be a region of zero delay, within the ECE time resolution of 0.05 ms.

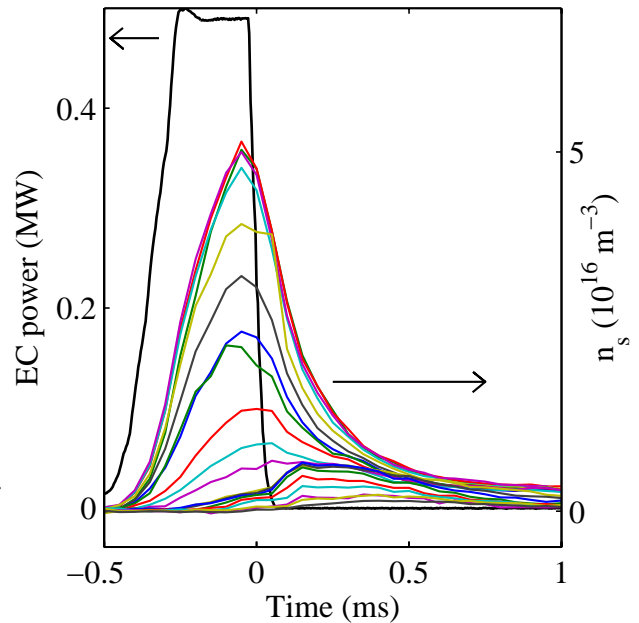


Fig. 1 Suprathermal density derived from the HFS ECE signals, in response to a short central ECCD pulse with a toroidal injection angle of 25° (ending at $t=0$), averaged over 114 coherent pulses (shot 25018, current $I_p = 230$ kA, line-averaged density $\bar{n}_e = 1.5 \times 10^{19} \text{ m}^{-3}$, peak temperature $T_b = 1.5$ keV, edge elongation $\kappa = 1.6$).

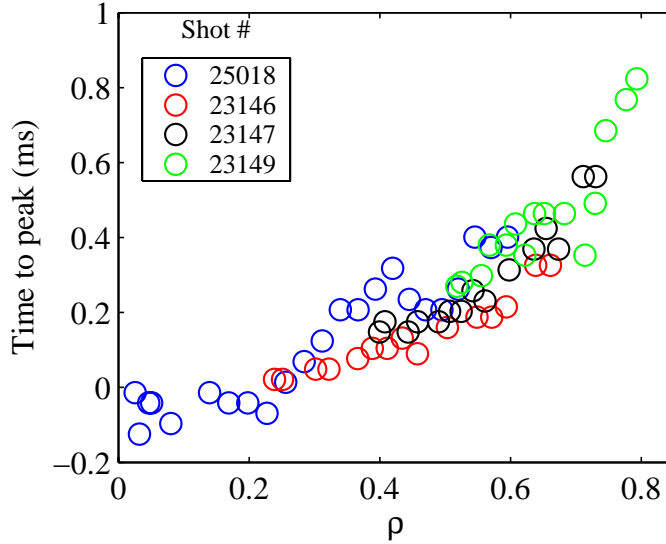


Fig. 2 Time lag from the end of a central ECCD pulse to the ECE peak, as a function of ρ (normalised radial coordinate proportional to the square root of the plasma volume), calculated by taking into account the estimated relativistic downshift, for four different shots ($I_p = 230$ kA, $\bar{n}_e = 1.5\text{-}2.1 \times 10^{19} \text{ m}^{-3}$, $T_b = 1.5$ keV, $\kappa = 1.6$, power = 0.45-0.9 MW)

The effect of radial transport on the shape of the suprathermal profile is rendered readily apparent by plotting successive snapshots of the normalised n_s profile after $t=0$, as shown in Fig. 3 for a centrally heated and an off-axis heated case. In both discharges a substantial broadening of the profile around the deposition region is clearly observed. It is also apparent that the dynamics are rather complex and strongly space dependent, and would be difficult to describe, for instance, with a simple, purely diffusive model.

Part of the observed complexity may also be due to changes in the velocity distribution function over space and time, which even within the as-

sumptions of our simple model could be described by a non-uniform T_s profile with resulting changes in both the calculated n_s and the emission position of each channel. Ultimately, energy and position cannot be uniquely separated in the ECE signals without relying on constraints from models. However, it is preferable to proceed initially through model-independent analysis techniques in order to generate parameters that can eventually be employed in an objective evaluation of the goodness of different models.

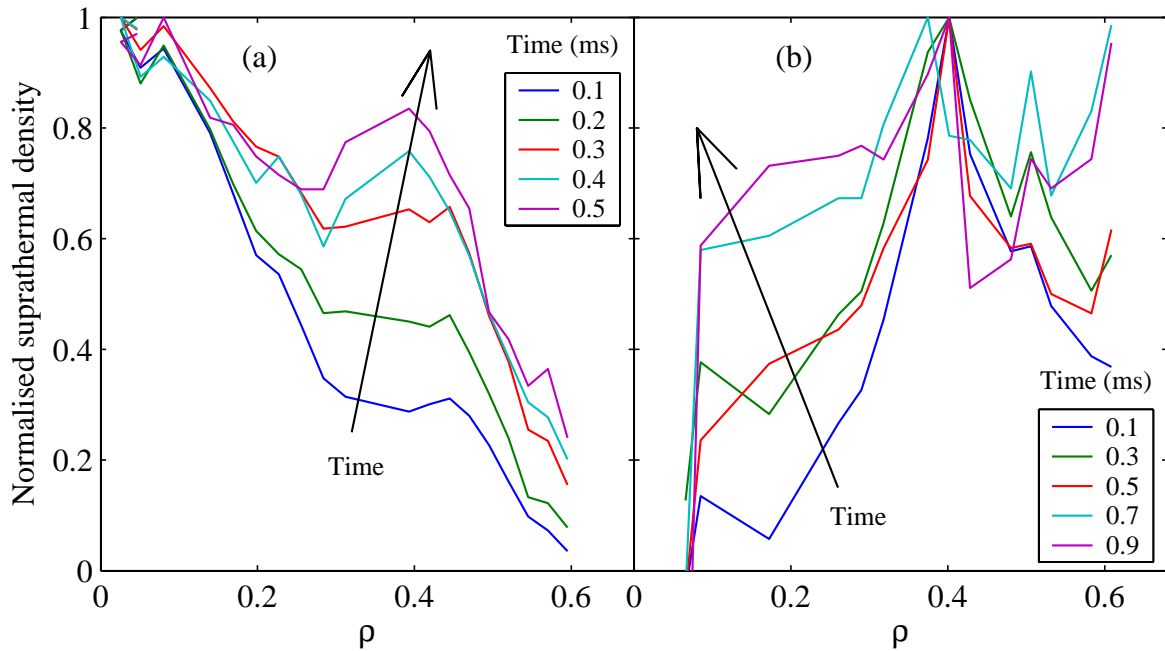


Fig. 3 Successive snapshots of normalised suprathermal density after ECCD turn-off: (a) shot 25018 (central deposition), (b) shot 23556 (deposition at $\rho \sim 0.45$). The plasma and EC parameters are similar (cf. Fig. 1).

A particularly satisfying approach is the determination of the transfer function of the system, in an eigenmode representation, by means of a formal system identification method [7]. We have performed a preliminary analysis of the discharges in this study, which include several parameter scans outside the scope of this paper, by assuming common poles for all ECE channels. Generally, a calculation with two or three poles yields optimal results, with no further improvement in the normalised loss function beyond a maximum of three. Results for two discharges are shown in Fig. 4. The eigenmodes are normalised such that their sum (also shown) represents an estimation of the source function. Figure 4(a) refers to the reference shot 25018; the case of Fig. 4(b) is identical except for the presence of 0.45 MW cw central pre-heating, with a resulting estimated $T_s \sim 20$ keV. In the latter discharge the source function is anomalously broad (an effect visible directly in the raw data).

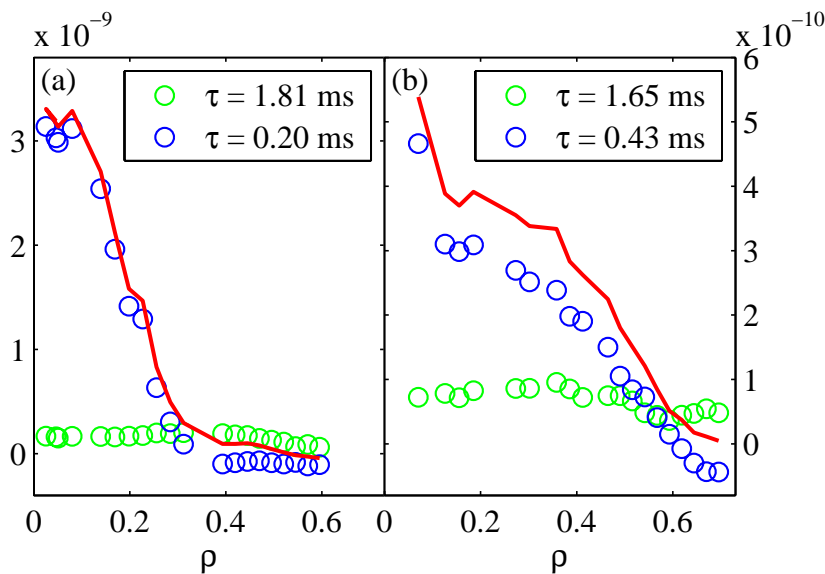


Fig. 4 Two-pole eigenmodes (circles) of the system transfer function (EC power to suprathermal density) and corresponding source functions (solid lines), for (a) shot 25018 (cf. Fig. 1), (b) shot 25032 (similar except for 0.45 MW cw central EC power, $T_b \sim 2$ keV). The time constant τ is given for each eigenmode.

These results amply illustrate the potential of this technique in determining the suprathermal electron source function and the characteristic time constants of the relevant dynamical processes. The next stage of this analysis will be the application of specific transport models to these eigenmode sets.

These results amply illustrate the potential of this technique in determining the suprathermal electron source function and the characteristic time constants of the relevant dynamical processes. The next stage of this analysis will be the application of specific transport models to these eigenmode sets.

Acknowledgment

This work was supported in part by the Swiss National Science Foundation.

References

- [1] S. Coda et al., Proc. 19th Int. Conf. on Fusion Energy, Lyon, 2002, EX/W-5 (IAEA, to be published); S. Coda et al., submitted to Nucl. Fusion (2002).
- [2] P. Nikkola et al., submitted to Nucl. Fusion (2002).
- [3] T.P. Goodman et al., Proc. 19th Conf. on Fusion Energy, Lyon, 2002, OV/4.2 (IAEA, to be published).
- [4] P. Blanchard et al., Plasma Phys. Control. Fusion **44** (2002) 2231.
- [5] M. Bornatici et al., Nucl. Fusion **23** (1981) 1127.
- [6] K. Matsuda, IEEE Trans. Plasma Sci. **17** (1989) 6.
- [7] J.-M. Moret and Equipe Tore Supra, Nucl. Fusion **32** (1992) 1241.